ATTENUATION OF SOUND IN SOME OVERLOADED ABSORBERS BY A PULSE TECHNIQUE

Thesis for the Degree of M. S.

MICHIGAN STATE UNIVERSITY

Jay H. Wolkowisky

1961

This is to certify that the

thesis entitled

ATTENUATION OF SOUND IN SOME OVERLOADED ABSORBERS BY A PULSE TECHNIQUE

presented by

JAY H. WOLKOWISKY

has been accepted towards fulfillment of the requirements for

MASTER OF SCIENCE degree in APPLIED MECHANICS

Clement A. Tatro
Major professor

Date May 5, 1961

O-169

ABSTRACT

ATTENUATION OF SOUND IN SOME OVERLOADED ABSORBERS BY A PULSE TECHNIQUE

by Jay H. Wolkowisky

The main purpose of this study is to investigate the sound absorption properties of some rubber-like and elastic materials as a function of the frequency and of the stress.

A predetermined static stress is applied to a specimen through long transmitter rods, by means of a universal testing machine. A stress pulse is produced which travels through the specimen. By means of strain gages, the strain pulse can be recorded before it enters and after it leaves the specimen.

The input and output pulses are represented by a finite Fourier series. By using this series in a Fourier Integral the amplitude distribution function for each of the input and output pulses is obtained. Calculating the ratio of the mean squared (over small frequency bands) amplitude distribution functions for the input and output pulses, a measure of the energy transmission is obtained. By varying the static load applied to the specimen, the dependence of the energy transmission on the static stress is obtained.

The results are plotted as histograms. These show that the more rubbery a material is the more the sound absorption properties change with stress. Also that at certain frequencies there is resonance phenomenon for some of the materials tested.

ATTENUATION OF SOUND IN SOME OVERLOADED ABSORBERS BY A PULSE TECHNIQUE

By

Jay H. Wolkowisky

A THESIS

Submitted to
Michigan State University
in partial fulfillment of the requirements
for the degree of

MASTER OF SCIENCE

Department of Applied Mechanics

1961

ACKNOWLEDGEMENTS

I wish to express my gratitude to Dr. C. A. Tatro, who originally suggested the problem and for his assistance in solving the experimental problems encountered. I am also grateful for the advice given to me by other members of the faculty.

Sincere thanks are also due to Mr. J. W. Hoffman and the Division of Engineering Research for their cooperation and support of this work.

I also wish to express my gratitude to Mr. D. H. Yen for his valuable assistance in devising the program for the "Mistic" electronic computer.

I would also like to thank Mr. R. W. Jenkins and Mr. E. A. Thompson for their assistance in building the apparatus.

CONTENTS

LIST OF FIGURES

LIST OF FIGURES CONTINUED

LIST OF SYMBOLS

$A'(\omega) = A(f)$	=	Amplitude Distribution Function (Fourier Integral Transform)
a_i	=	ordinate for amplitude distribution function for output pulse
B_{mi}	=	six by six transformation matrix
b_i	=	i^{th} coefficient of the finite Fourier series representation of f(t)
c_j	=	ordinate for amplitude distribution function for input pulse
f_i	=	$f(\frac{iL}{n})$
f(t)	=	strain pulse (input or output) $0 \leq t \leq L$
f	=	frequency (cycles/sec)
i, j, m	=	indices (integers)
L	=	temporal wave length of f(t)
n	=	number of terms of finite Fourier Series
$\overline{P}_i$	=	incident average power per unit area
$\overline{P}_r$	=	reflected average power per unit area
R_f	=	mean squared amplitude distribution ratio for frequency band centered at f
t	=	time
V_1	=	elastic wave velocity of first medium
V_2	=	elastic wave velocity of second medium
ρ_1	=	mean density of first medium
ρ_2	=	mean density of second medium
ω	=	$2\pi f$

CHAPTER I

INTRODUCTION AND REVIEW OF PAST WORK

This investigation was inspired by the need to select a material exhibiting good sound isolation properties while under severe compressive stresses. The material is to be used in isolating tensile specimens from the load holders of a testing machine in Acoustic Emission studies (Ta 60).

The present analysis attempts to determine the sound deadening power of a material while under a load. In other words, the material is being tested under the same conditions as would be experienced by it in actual practice.

The analysis is based solely on the comparison of the input and output shapes of a transient stress wave. This transient stress wave is measured before it enters and after it leaves the specimen (the method of measurement will be explained in the next chapter). Therefore, since the pulse is not actually being measured in the specimen, what is being measured is the combined effects of two important mechanisms of energy dissipation. These two mechanisms will now be explained. They are first, the loss of energy of the incident pulse due to reflection at the interfaces; and second, the attenuation due to internal friction.

<u>Reflection at the interfaces</u>: Looking at the equation (Li 60),

$$\overline{P}_r = \left[\frac{1 - \dfrac{\rho_2 V_2}{\rho_1 V_1}}{1 + \dfrac{\rho_2 V_2}{\rho_1 V_1}} \right] \overline{P}_i$$

it is seen that if $\rho_2 V_2 >> \rho_1 V_1$ or $\rho_1 V_1 >> \rho_2 V_2$, then $\overline{P}_r \approx \overline{P}_i$, or practically all the energy is reflected. Also, it is seen from this equation that if $\rho_2 V_2 = \rho_1 V_1$ none of the energy is reflected.

If the media are well matched, (ρV values are close together) then considerable energy transmission takes place. If the media are badly matched (ρV values differ greatly), then there is a corresponding poor energy transmission. So it is clear that the quantity ρV, called the "specific acoustic resistance", controls the transmission of energy at an interface from one medium to another. Therefore, for a good isolator, it would be advantageous to have the specific acoustic resistances differ greatly.

Internal friction: There is at present no satisfactory theory of internal friction in solids, and more experimental data are required. Internal friction in solids may be produced by several different mechanisms, and although these all result in the mechanical energy being transformed into heat, two different dissipative processes are involved. These two processes are roughly analogous to the viscosity losses and thermal conduction losses in the transmission of sound waves through fluids. These processes will not be discussed further, since a study of the mechanism of internal friction was not the main objective of this investigation.

In this analysis the effects of reflection and internal friction will not be considered separately. The total effect of these two mechanisms will be lumped together and this total energy loss will be analysed. The methods which have been used previously to measure energy dissipation in solids may be divided into several classes, these are:

1. Free vibration methods
2. Resonance methods
3. Wave-propagation methods

This investigation can be classified with the wave propagation methods, but yet the method of analysis is quite different from what has been done before.

1. Free Vibration Methods. This method is most suitable for materials which are linear. At a given frequency of oscillation the period and logarithmic decrement of free oscillations can be measured. From these measurements its mechanical properties and behavior can be found.

2. Resonance Methods. This method is based on the principle that if an oscillating force, whose amplitude is fixed but whose frequency can be varied, is applied to a material, the amplitude of the resulting vibration passes through a maximum at a frequency which is known as the resonant frequency of the system. The value of this resonant frequency depends on the elastic properties of the system, while the width of the resonance peak gives measure of the dissipative forces which are present.

3. Wave-Propagation Methods. When a stress wave is propagated through a solid, and the solid is not perfectly elastic, some of the energy of the stress wave is dissipated as it passes through the medium. The attenuation can be measured and from known relationships (Ko 53) a measure of the internal friction can be determined. The experiment used in this investigation is based on the same principle but the method of analysis to determine the relative energy dissipation at various frequencies is strictly a mathematical one.

Work on the propagation of low frequency longitudinal waves in filaments has been mainly concerned with the dynamic behavior of rubber-like materials and high polymers. Some of these investigations have been done by Ballou and Silverman (Ba 44), Nolle (No 48), Ballou and Smith (Ba 49), Hillier and Kolsky (HiK 50), and Hillier (Hi 50).

Another technique using the propagation of waves has been to produce a short pulse of high-frequency oscillation and measure its time of transit and its attenuation as it passes back and forth along the specimen. This method is similiar to the principle used in radar. Ivey, Mrowia, and Guth (Iv 49) have used this technique to work with rubber specimens.

More recently Auberger and Rinehart (Au 61) have used an electrosonic pulse technique developed by Hughes (Hu 49) to investigate the attenuation of stress waves in plastics.

All these investigations have been primarily concerned with obtaining data on internal friction. This investigation differs slightly in that its main purpose is not so much to obtain quantitative results but to explain a possible method of analyzing an attenuated stress pulse and to obtain an over-all picutre of sound absorption as a function of frequency without analyzing the details responsible for it. As a consequence, all results have been represented graphically.

CHAPTER II

DESCRIPTION OF EXPERIMENT

The experimental apparatus is very simple and is depicted in Fig. 1. The stress wave is produced by a short steel striker rod (a) which falls under its own weight and hits the upper end of a one inch diameter circular steel bar (b). The striker rod is guided in its fall by a pipe (c) which has an inside diameter approximately the same size as the outside diameter of the striker rod. The striker has a light nylon line (d) attached to its top end so that it can be pulled to the desired height again for the experiment to be repeated.

The stress wave travels down the upper bar, passes through the specimen (e) and travels into the lower steel bar (f). The specimens are all about 1/8" thick. The upper bar is held in place by a collar (g) which is attached to the stationary head of the testing machine. All the contact surfaces between the collar and the upper bar are separated with a soft material so that there will be as little interference as possible with the stress wave as it travels down the upper bar.

Two sets of type A-8 strain gages are used. One set (h) to measure the stress wave before it enters the specimen and the other set (i) to measure it after it has left the specimen. Each set consists of four gages. Two are used to measure the lateral strain and are placed 180° apart on the bar. The other two in the set are used to measure the longitudinal strain and are also placed 180° apart. The four strain gages in each set are hooked up in a bridge circuit so that the strain measured will be a sum of the four individual strains. The wiring is described in Figs. 2, 3, 4. The strain gage set on the upper bar is approximately one striker bar length from the specimen so that the stress wave will have completely passed through these strain gages before the reflection has a chance to interfere. The set of strain gages on the lower bar are placed approximately one striker bar length from its lower end so that the reflections from the welded joint do not interfere as the stress wave passes through these gages.

The upper bar is quite long (three feet) since it is desirable to have the strain gages far from the struck end of the bar. This is so that the transient end effects produced when the striker hits the bar will die out before they reach the strain gages and therefore not interfere with the main pulse.

A crystal (j) is used to trigger the first oscilloscope. This is placed about seven inches above the top set of strain gages. An external trigger is needed for the first oscilloscope since the entire pulse had to be recorded. The external trigger serves the purpose of triggering the sweep before the stress wave actually reaches the strain gages. The sweep of the second oscilloscope is triggered from the first for the same reason.

As can be seen from Fig. 1 the lower bar is attached to the movable lower head of the testing machine. The compressive load is applied to the specimen when the lower head of the testing machine moves up.

The oscilloscopes used were Tektronix units with Dumont Type cameras attached to photograph the pulses which are projected on the oscilloscope screen.

Now for a summary of the experiment. The testing machine applies the predetermined static load to the specimen. The striker hits the upper bar, the stress wave travels down the bar to the first set of strain gages and the resulting strain pulse is photographed from the screen of the first oscilloscope. The wave continues through the specimen and the resulting strain pulse is picked up by the second set of gages and photographed. These input and output photographs are the data to be analyzed.

The experiment was done with sheets of nine different materials: white felt, neoprene, nylon, silicon rubber, teflon, saran, clay impregnated bakelite, red rubber, and hard board. These materials were thought to have good sound absorption properties and also meet other design criteria. Each of these materials were tested under three different static loads: 500 lbs., 1500 lbs., 4000 lbs. These loads correspond to static stress in the specimens of 636 psi., 1910 psi., and 5100 psi. respectively.

Due to the fact that the analysis of the data is such a lengthly process, only three of the materials (white felt, neoprene, nylon) were analyzed under loads of 1500 lbs. and 4000 lbs. each. The data not processed is on file with the Applied Mechanics Department, Michigan State University.

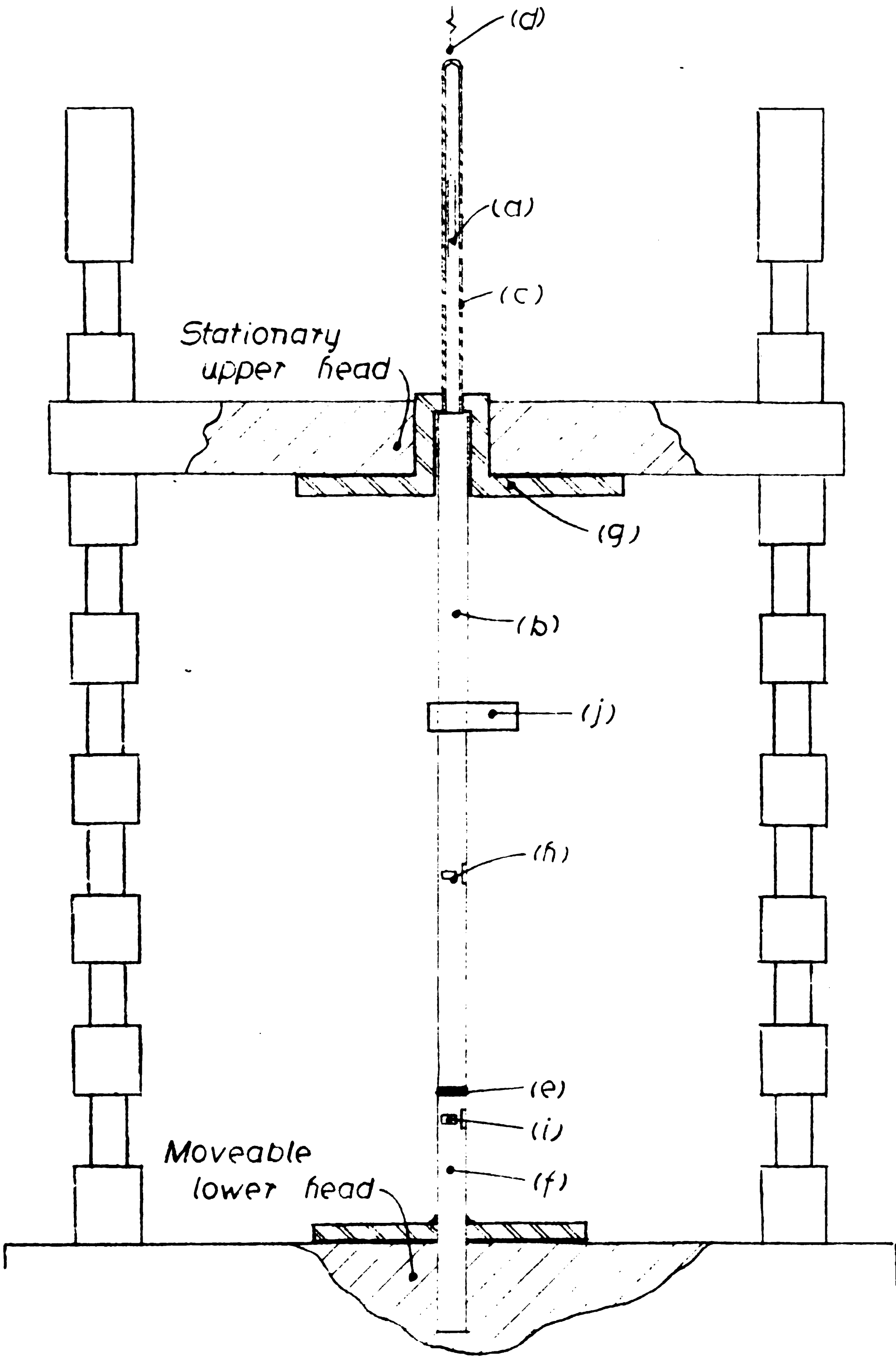

MECHANICAL APPARATUS

FIGURE 1

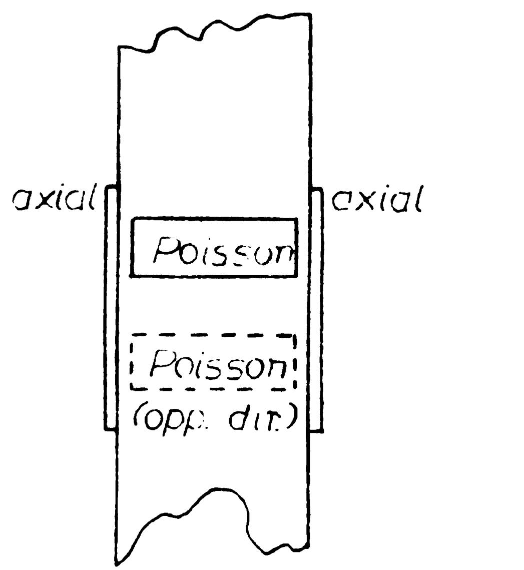

Gages are BLH type A-8,
R-120Ω., GF=1.83.

GAGE PLACEMENT

FIGURE 2

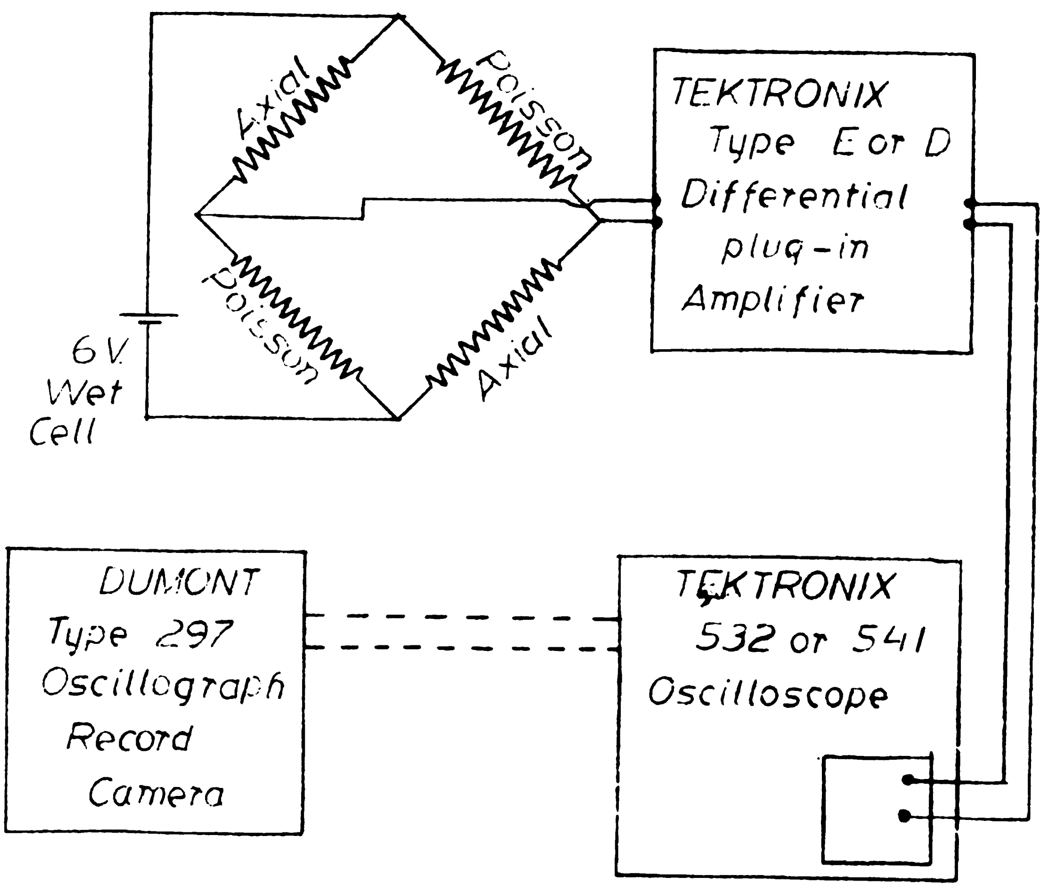

FUNCTIONAL BLOCK DIAGRAM FOR EACH BRIDGE

FIGURE 3

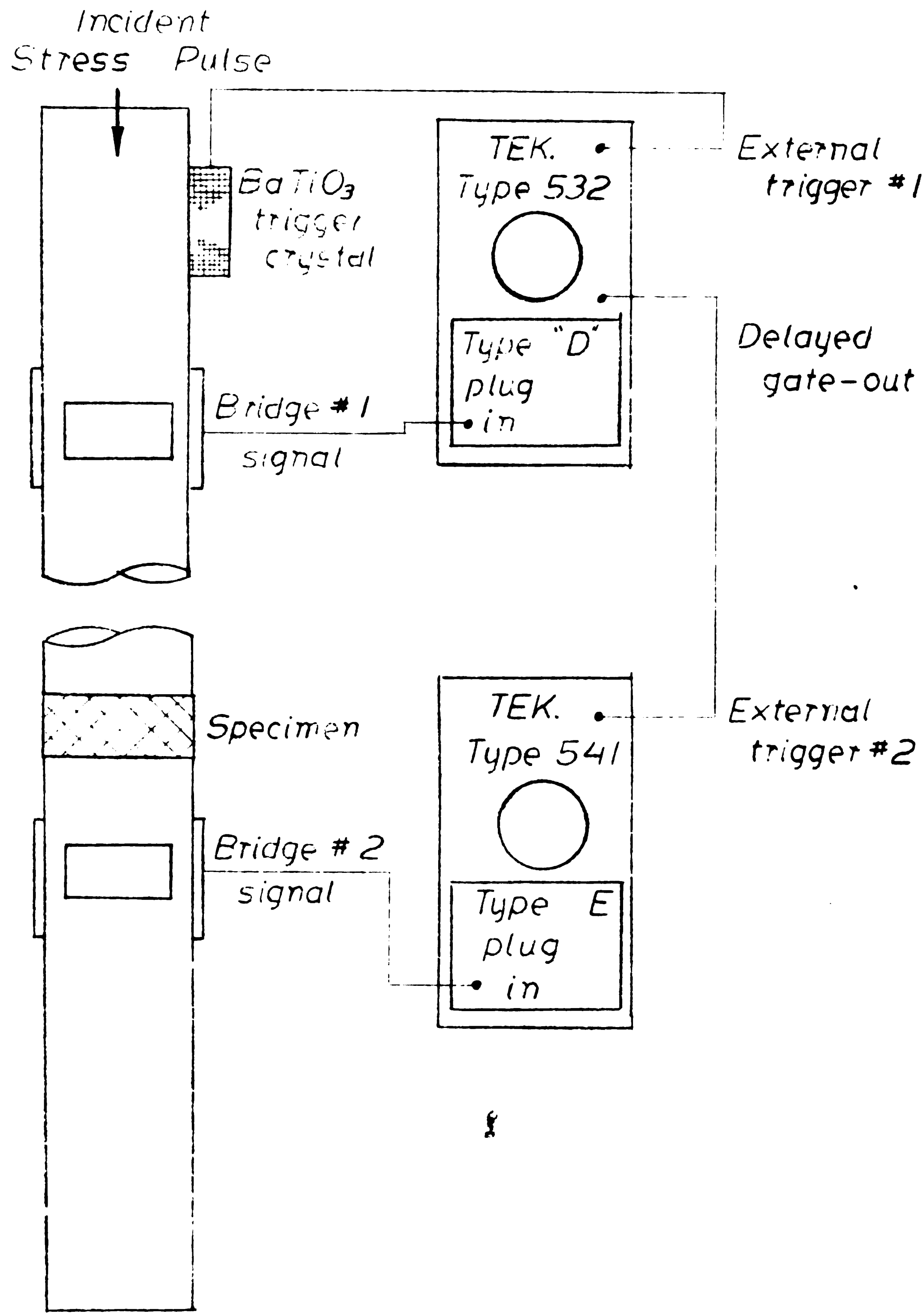

SCHEMATIC DIAGRAM SHOWING METHOD OF TRIGGERING

FIGURE 4

CHAPTER III

ANALYSIS OF THE DATA

A set of data will be considered as the two photographs of the input and output pulses from one run of the experiment; four sets of such photographs are shown in Fig. 5. A pulse is represented in Fig. 6 by f(t). The pulse for $0 \leq t \leq L$ will be represented by a finite Fourier series. In doing this the wiggles of the pulse for $t > L$ will be neglected. These parts of the pulse, represented by dotted lines in Fig. 6, are due to dispersion of components of higher frequencies than were of interest here. This approximated pulse will be called f(t). It has been shown (Wh 54) that a given function can be represented by a sum of sine terms:

$$f(t) = b_1 \sin \frac{\pi t}{L} + b_2 \sin \frac{2\pi t}{L} + \quad \ldots . \; b_n \quad \frac{\sin (n - 1) \pi t}{L}$$

which will take given values for (n - 1) given equally spaced values of the argument t; say

$$f(\frac{L}{n}) = f_1 \;, \; f(\frac{2L}{n}) = f_2 \;, \; \ldots . \; f \; \frac{(n - 1) L}{n} = f_{n-1}$$

where f_1, f_2 ..... f_{n-1} are given numbers, and the coefficients are given by

$$b_i = \frac{2}{n} \left\{ f_1 \sin \frac{i\pi}{n} + f_2 \sin \frac{2i\pi}{n} + \quad \ldots . \; f_{n-1} \sin \frac{(n - 1)i\pi}{n} \right\}$$

For our case $n = 7$ and hence

$$f(t) = \sum_{i=1}^{6} b_i \sin \frac{i\pi t}{L} \qquad (1)$$

where

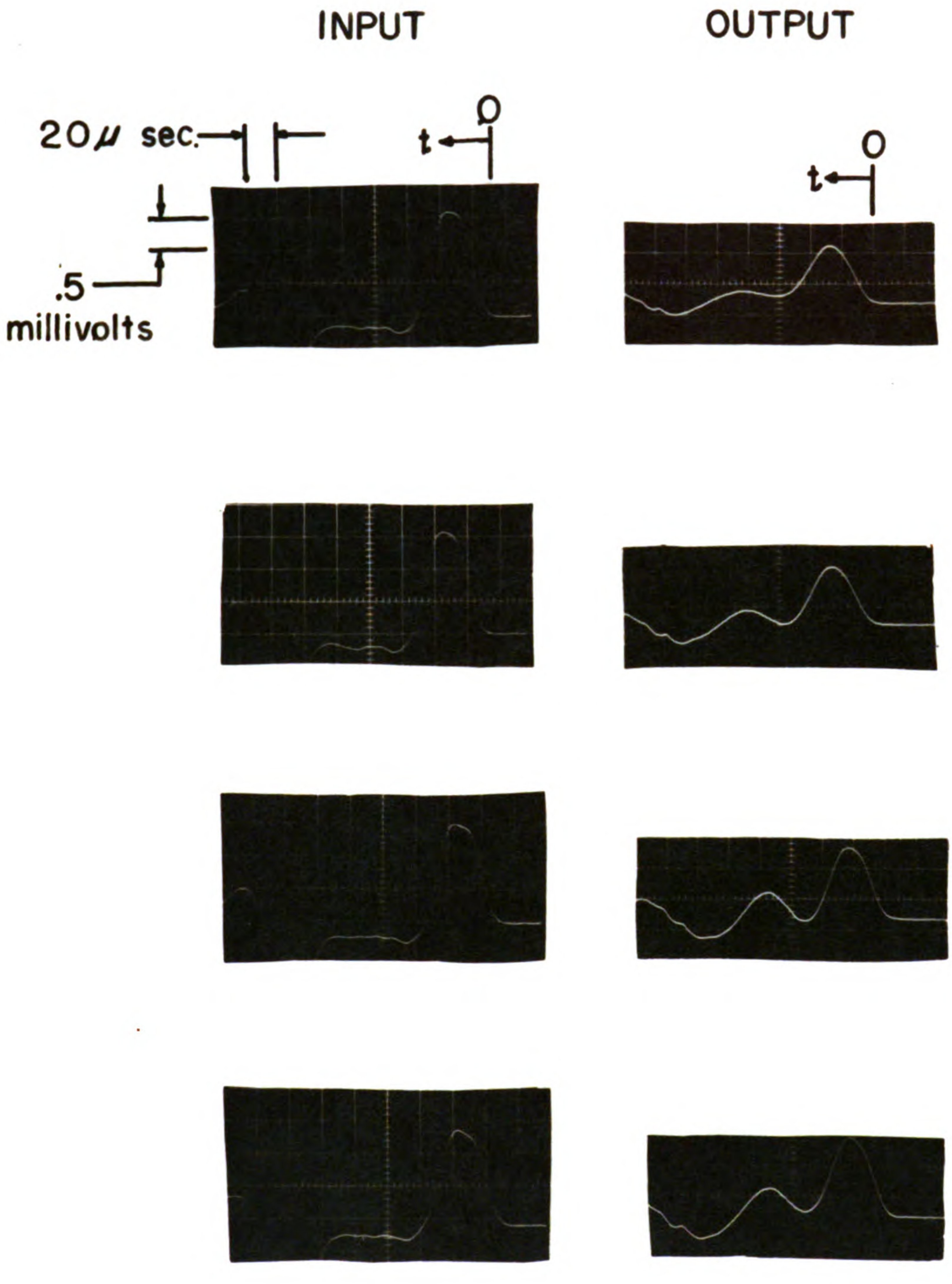

FIGURE 5 - Some Typical INPUT and OUTPUT Strain Pulses

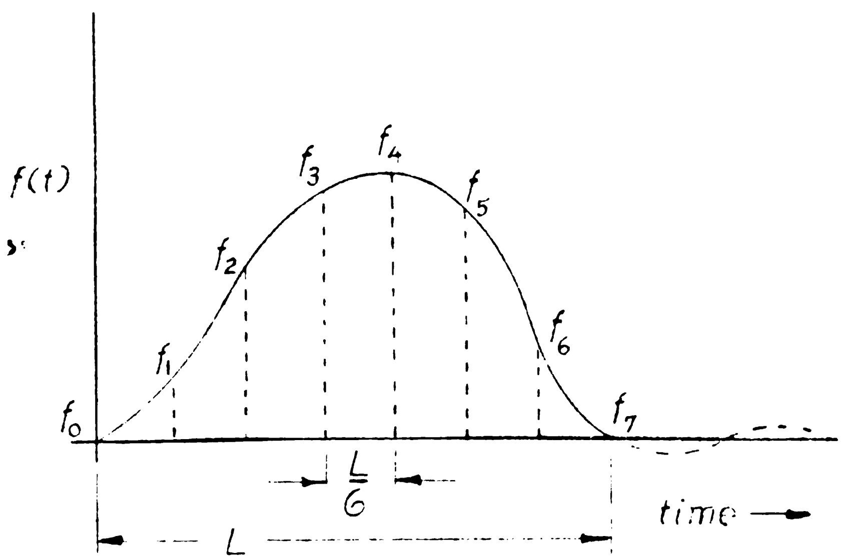

Symbolic Diagram of a Strain Pulse

FIGURE 6

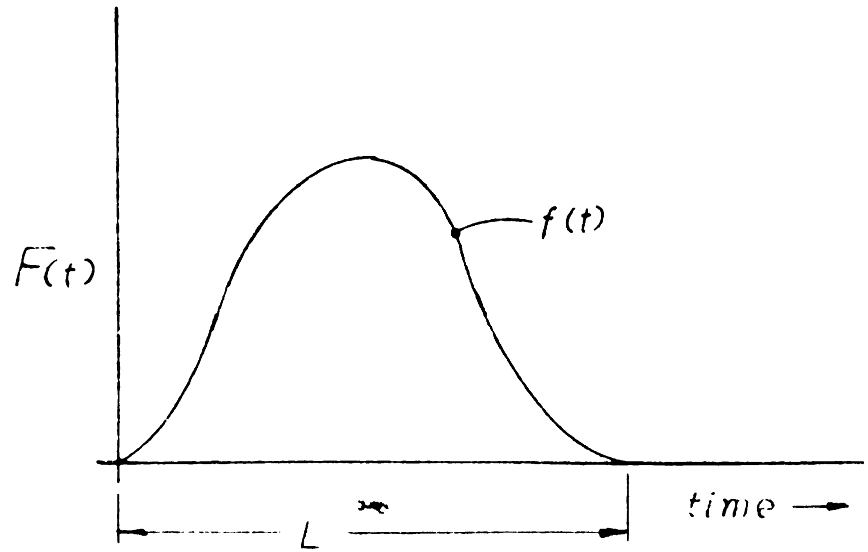

Symbolic Diagram for an Input or Output Function F(t)

FIGURE 7

$$b_i = \frac{2}{7} \sum_{j=1}^{6} f_j \sin \frac{j\, i\, \pi}{6} \tag{2}$$

The six equally spaced ordinates (f_j) of f(t) are measured directly from the photographs using a two-dimensional measuring microscope. The Michigan State University "Mistic" electronic computer was used to calculate the b_i's from equation (2). A completely new computer program had to be devised for this operation and is on file with the Applied Mechanics Department, Michigan State University.

If one thinks of the input pulse as a transient excitation of the system and the output pulse as the transient response, then one can treat the system almost as if it were a vibration problem. Since these input and output pulses are "random" (not a single monochromatic wave) then they can be represented as the sum of an infinite number of separate monochromatic waves. The function that tells "how much" of each separate wave is contained in the input and output pulses is just the Fourier integral transform (or amplitude distribution function) of these two pulses.

When the Fourier integral transform of these input and output pulses are taken they will be represented as functions of frequency. The pulses are now in a form in which they can be compared so that the results obtained will also be functions of the frequency. This is what was desired. The method for comparing the transformed input and output pulses will be explained later.

The equation for the Fourier integral will be developed. Since the same general method of using the transform will apply to both the input and output curves we can represent both of them by F(t) $0 \leq t < \infty$. As shown symbolically in Figure 7, the Fourier Integral representation is then

$$F(t) = \int_0^{\infty} A'(\omega) \sin \omega t \; d\omega$$

where

$$A'(\omega) = \frac{2}{\pi} \int_0^{\infty} F(t) \sin \omega t \; dt$$

This reduces to

$$A'(\omega) = A(f) = \frac{2L \sin 2\pi fL}{\pi^2} \sum_{i \; 1}^{6} \frac{b_i (-1)^i \, i}{4(fL)^2 - i^2} \qquad (3)$$

The details of the above calculation and method of plotting are given in the Appendix. These curves for A(f) are plotted in Figs. 8-13 for white felt, nylon, and neoprene at 1500 lbs. and 4000 lbs. each.

The transformed input and output curves are now compared in such a manner as to give the relative energy loss as a function of the frequency. This is done by taking the ratio of the mean squared (over small frequency bands) amplitude distribution function for the input and output pulse. This ratio will be called the "mean squared amplitude distribution ratio".

If R_f is this ratio for a frequency band "f", then

$$R_f = \frac{\sum_{i=1}^{n} a_i^2 / n}{\sum_{i=1}^{n} c_j^2 / n}$$

This is shown for a frequency band centered at f in Figure 14.

For this investigation a frequency band width of 5000 cycles/sec. and subintervals of width 1000 cycles/sec. was used. These ratios (R_f) are plotted as histograms in Figures 15 - 20.

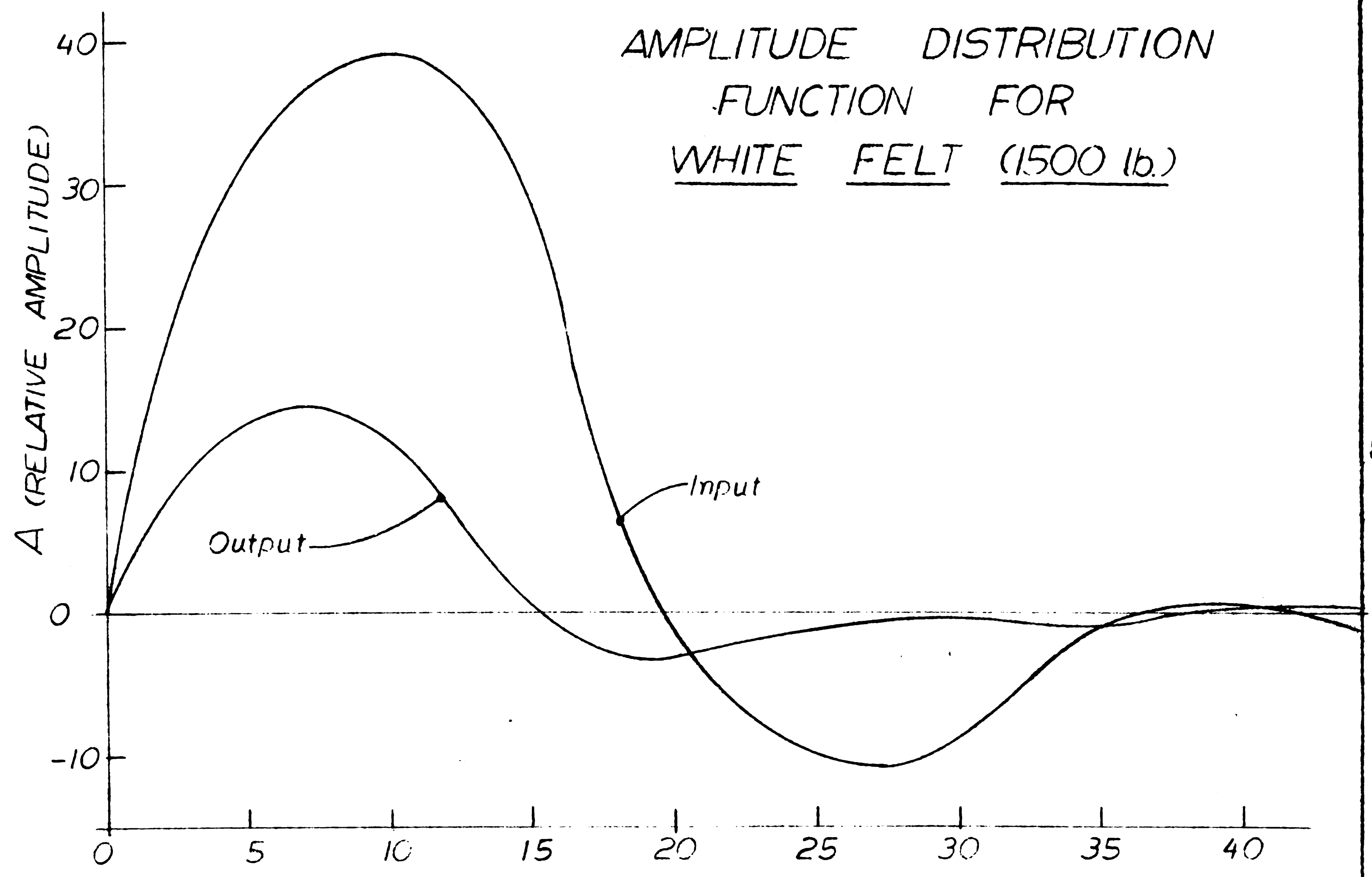
AMPLITUDE DISTRIBUTION
FUNCTION FOR
WHITE FELT (1500 lb.)
A (RELATIVE AMPLITUDE)
40
30
20
10
0
-10
Output
Input
0
5
10
15
20
25
30
35
40
FREQUENCY (kps)

FIGURE 8

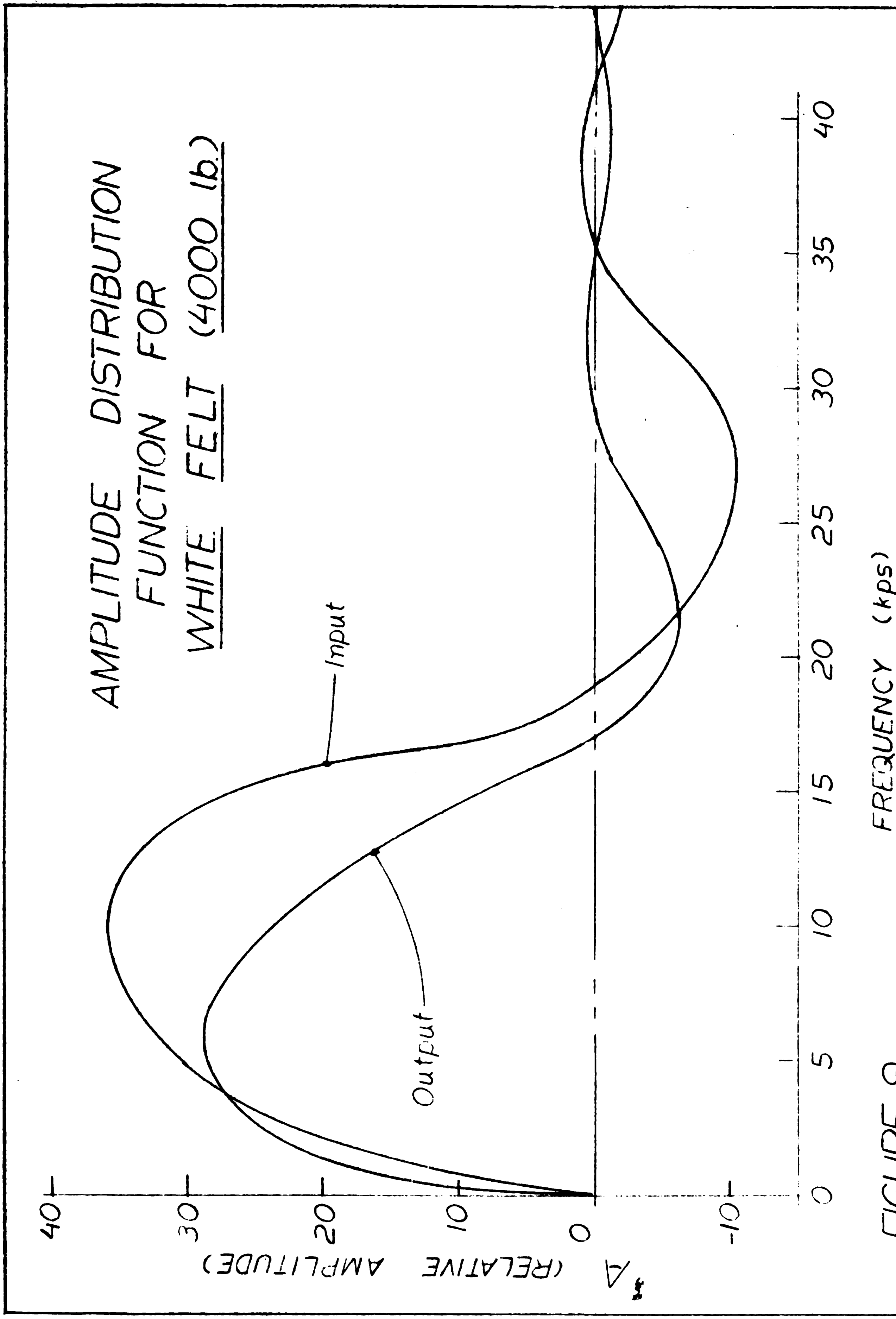
AMPLITUDE DISTRIBUTION FUNCTION FOR WHITE FELT (4000 lb.)
Input
Output
A_f (RELATIVE AMPLITUDE)
40
30
20
10
0
-10
0
5
10
15
20
25
30
35
40
FREQUENCY (kps)

FIGURE 9

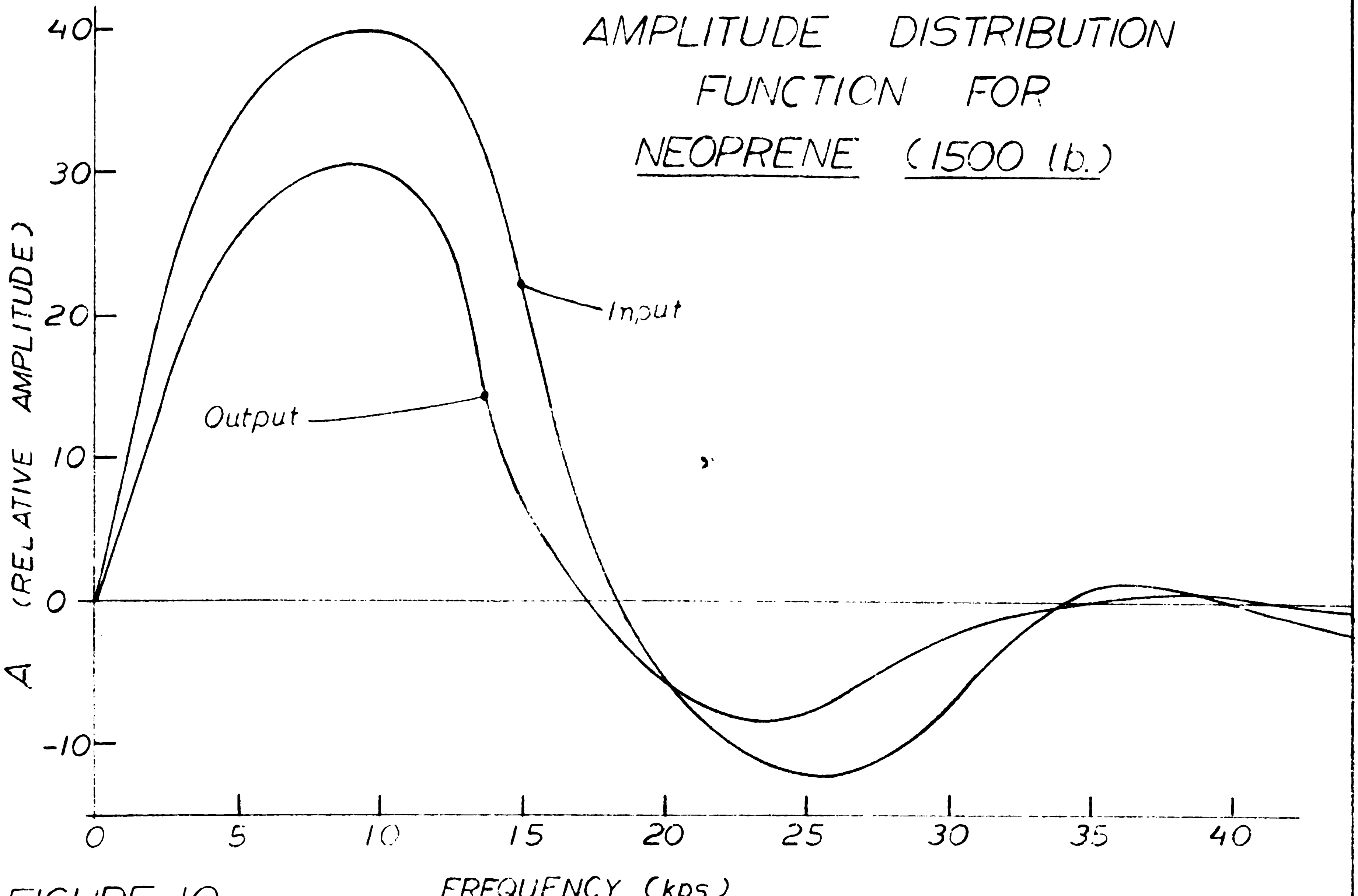
AMPLITUDE DISTRIBUTION FUNCTION FOR NEOPRENE (1500 lb.)
Input
Output
A (RELATIVE AMPLITUDE)
40
30
20
10
0
-10
0
5
10
15
20
25
30
35
40
FREQUENCY (kps)

FIGURE 10

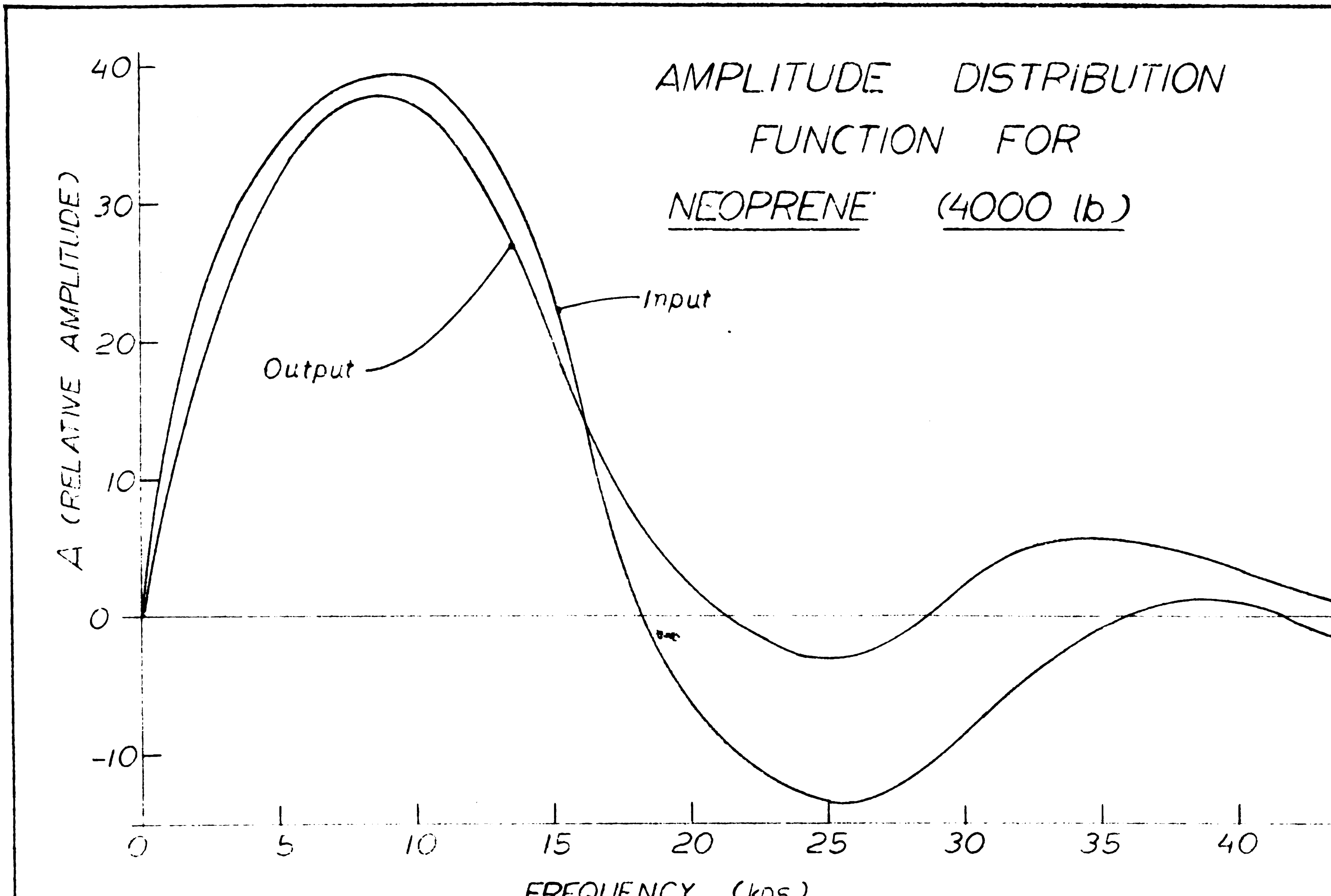
AMPLITUDE DISTRIBUTION
FUNCTION FOR
NEOPRENE (4000 lb)
A (RELATIVE AMPLITUDE)
40
30
20
10
0
-10
Input
Output
0
5
10
15
20
25
30
35
40
FREQUENCY (kps)

FIGURE 11

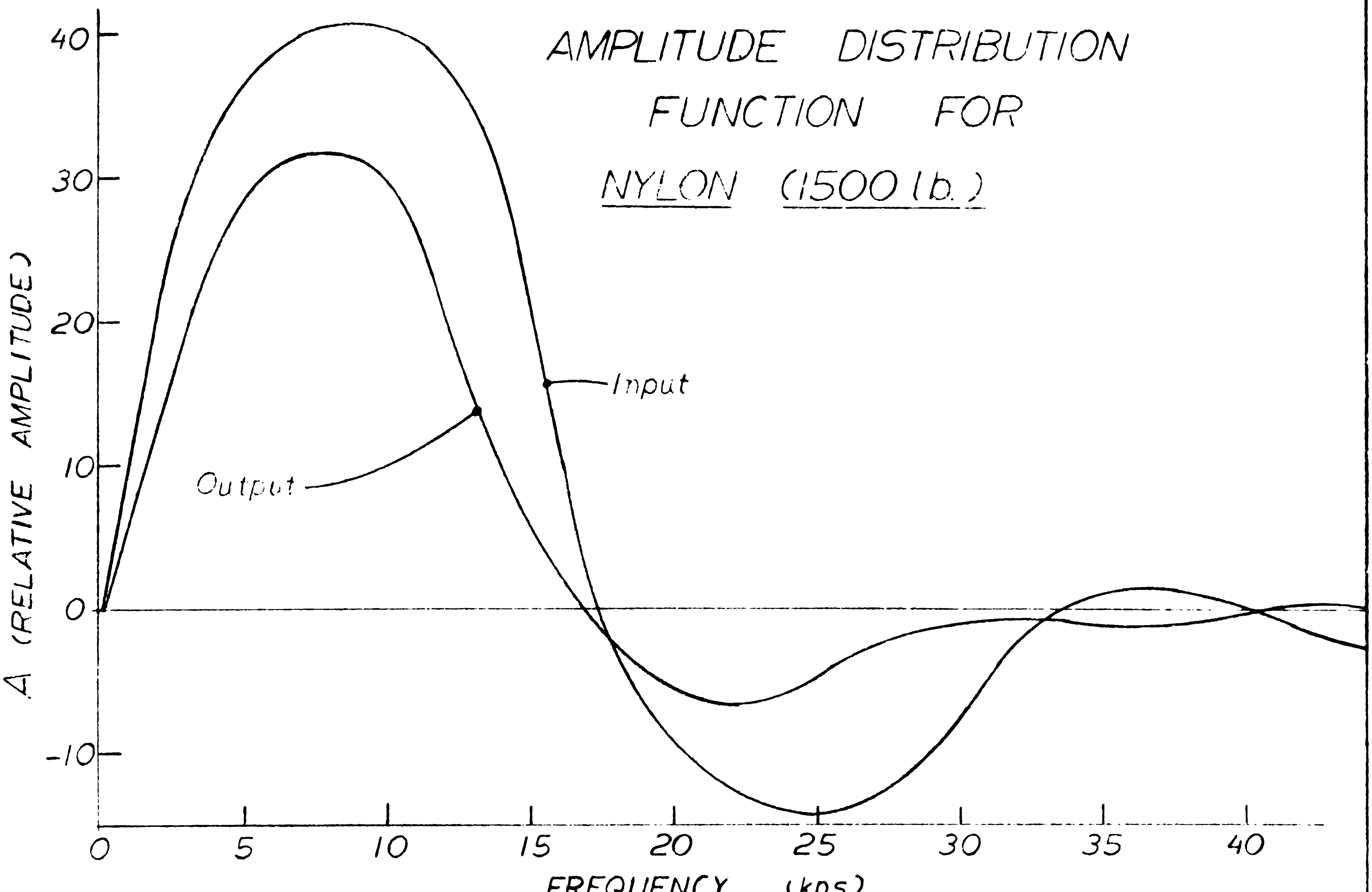
AMPLITUDE DISTRIBUTION
FUNCTION FOR
NYLON (1500 lb.)
40
30
20
10
0
-10
A (RELATIVE AMPLITUDE)
Input
Output
0
5
10
15
20
25
30
35
40
FREQUENCY (kps)

FIGURE 12

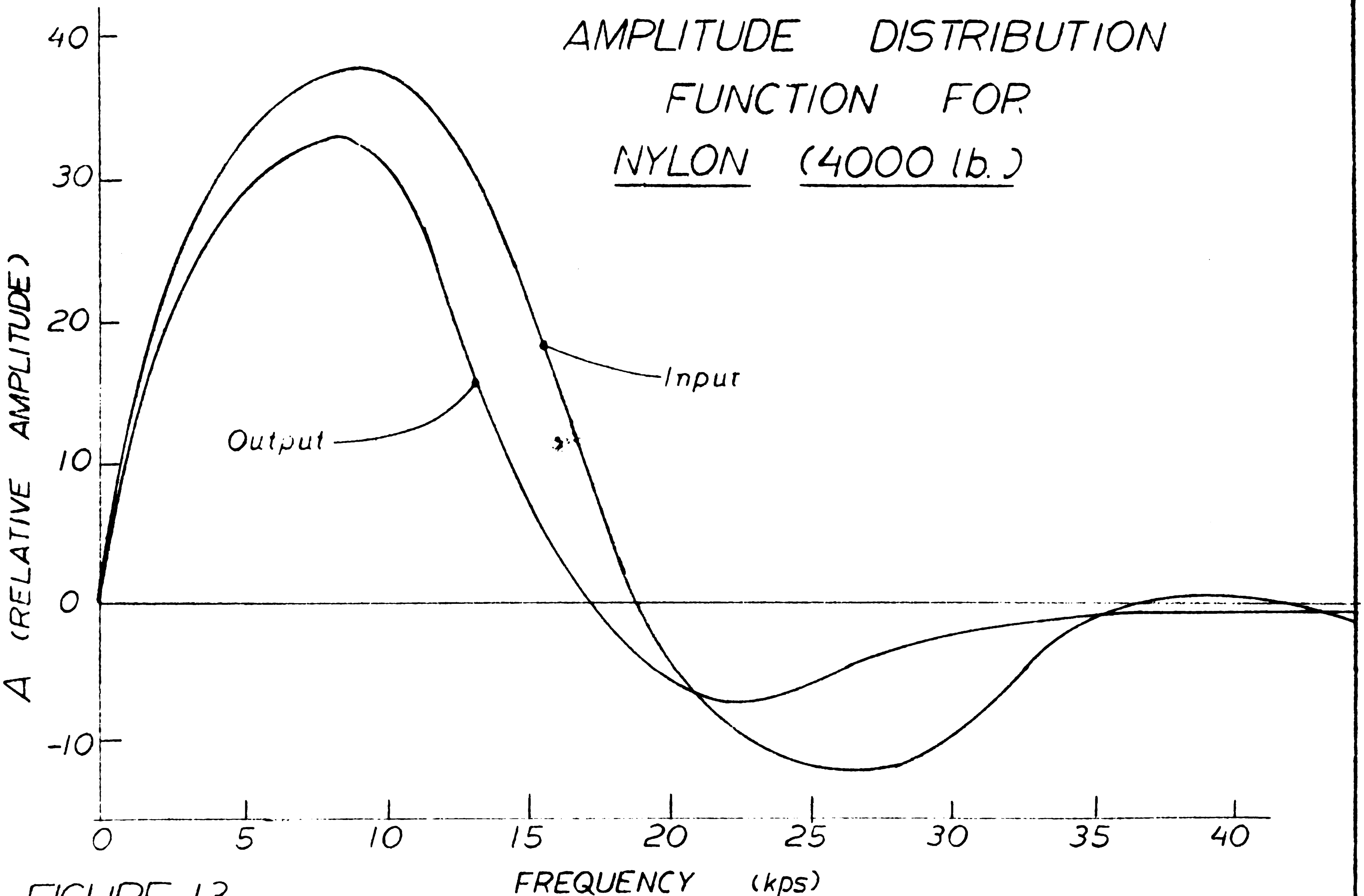
AMPLITUDE DISTRIBUTION
FUNCTION FOR
NYLON (4000 lb.)
A (RELATIVE AMPLITUDE)
40
30
20
10
0
-10
Input
Output
0
5
10
15
20
25
30
35
40
FREQUENCY (kps)

FIGURE 13

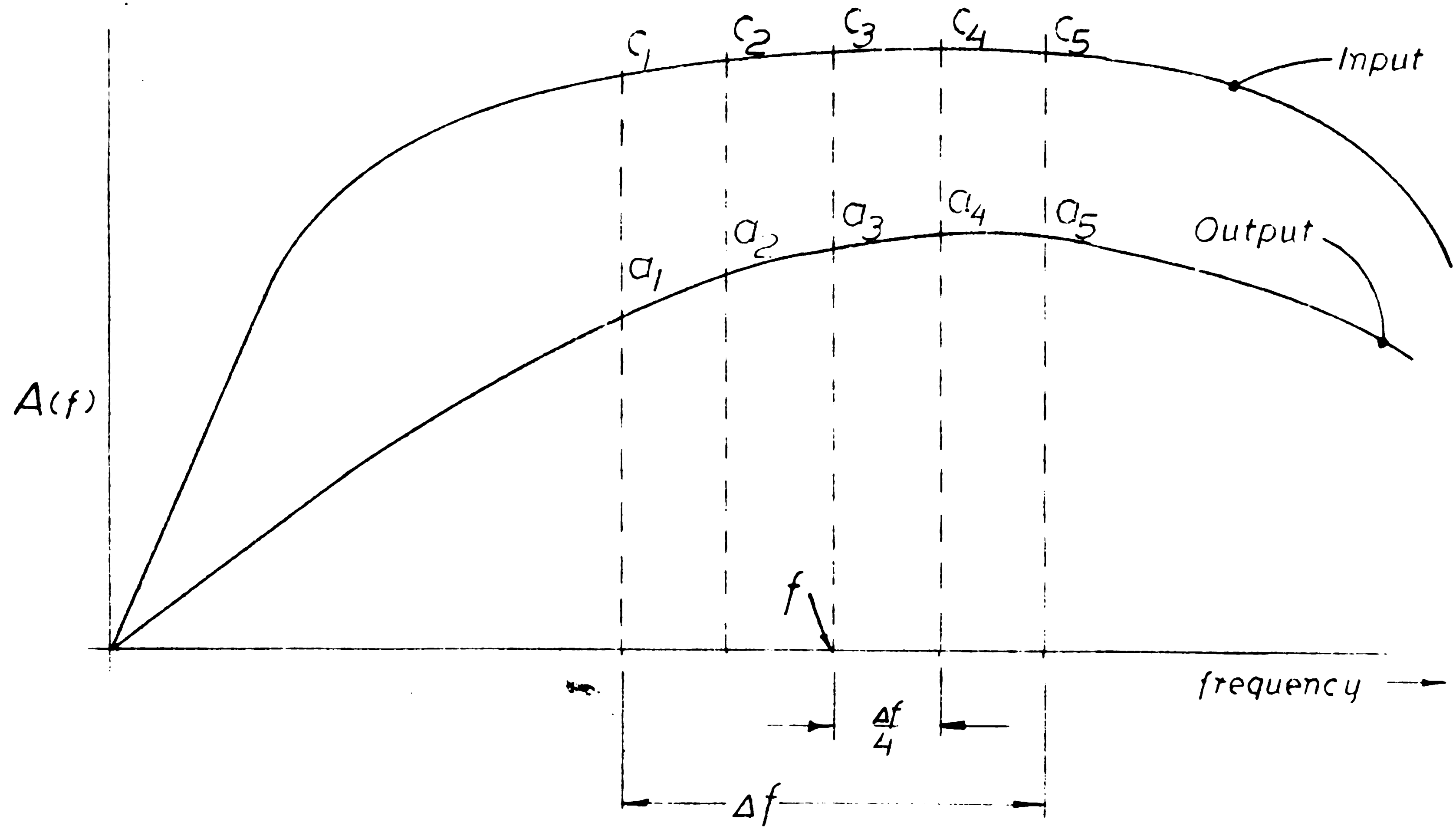

SYMBOLIC DIAGRAM OF HOW R_b IS CALCULATED.

FIGURE 14

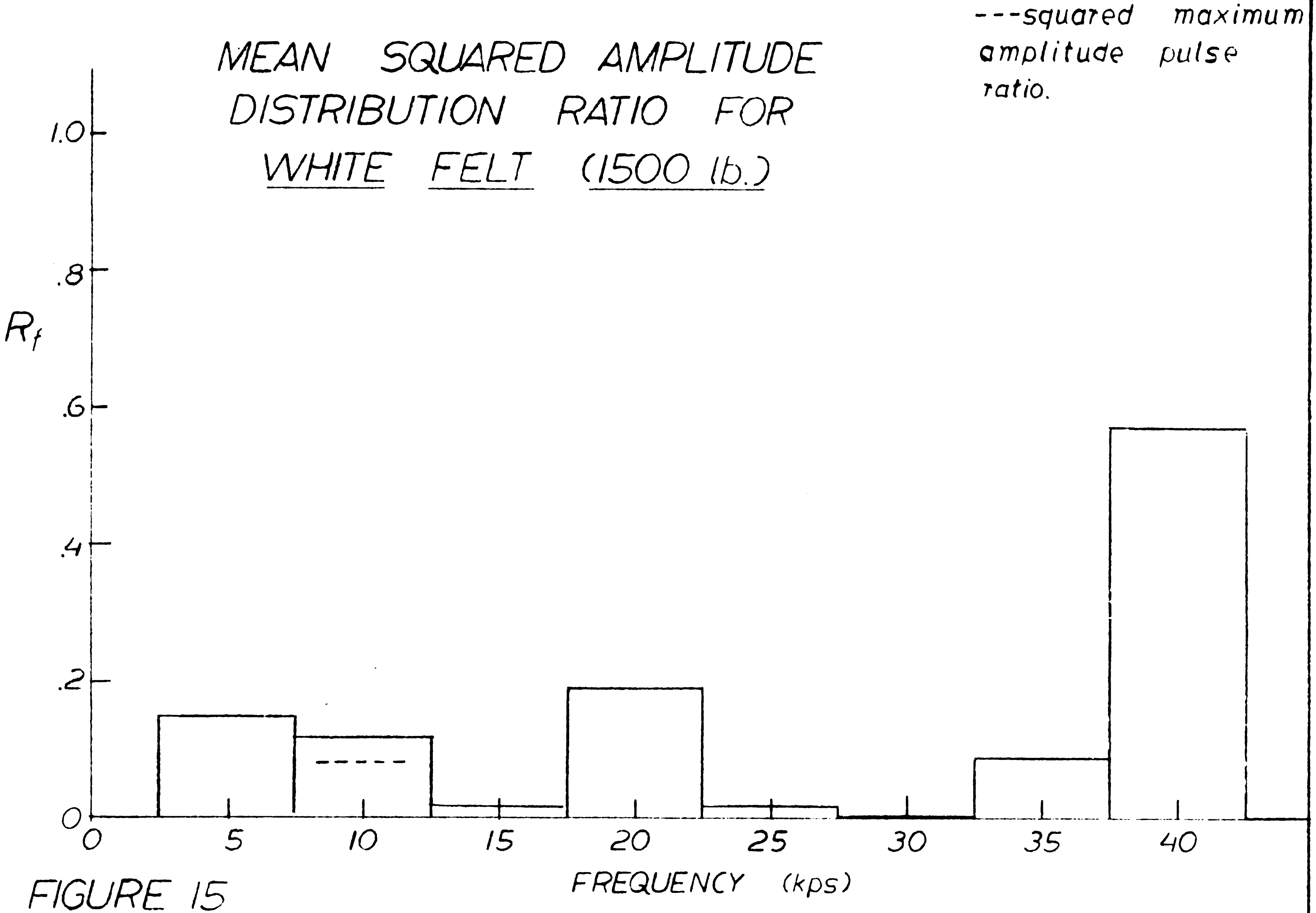
MEAN SQUARED AMPLITUDE DISTRIBUTION RATIO FOR WHITE FELT (1500 lb.)
---squared maximum amplitude pulse ratio.
R_f
1.0
.8
.6
.4
.2
0
0
5
10
15
20
25
30
35
40
FREQUENCY (kps)

FIGURE 15

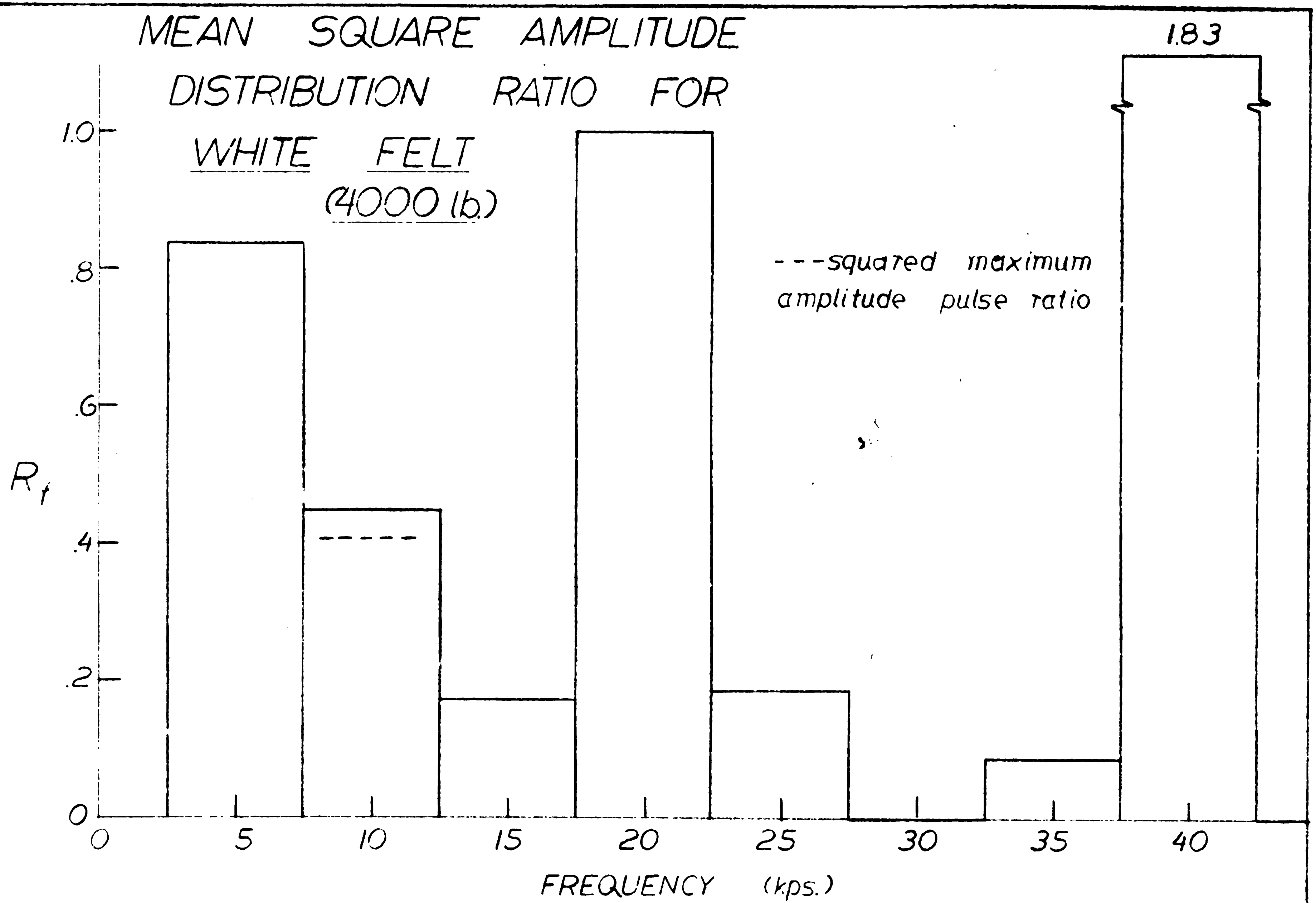
MEAN SQUARE AMPLITUDE
DISTRIBUTION RATIO FOR
WHITE FELT
(4000 lb.)
1.83
---squared maximum
amplitude pulse ratio
R_f
1.0
.8
.6
.4
.2
0
0
5
10
15
20
25
30
35
40
FREQUENCY (kps.)

FIGURE 16

MEAN SQUARED AMPLITUDE DISTRIBUTION RATIO FOR NYLON (1500 lb.)

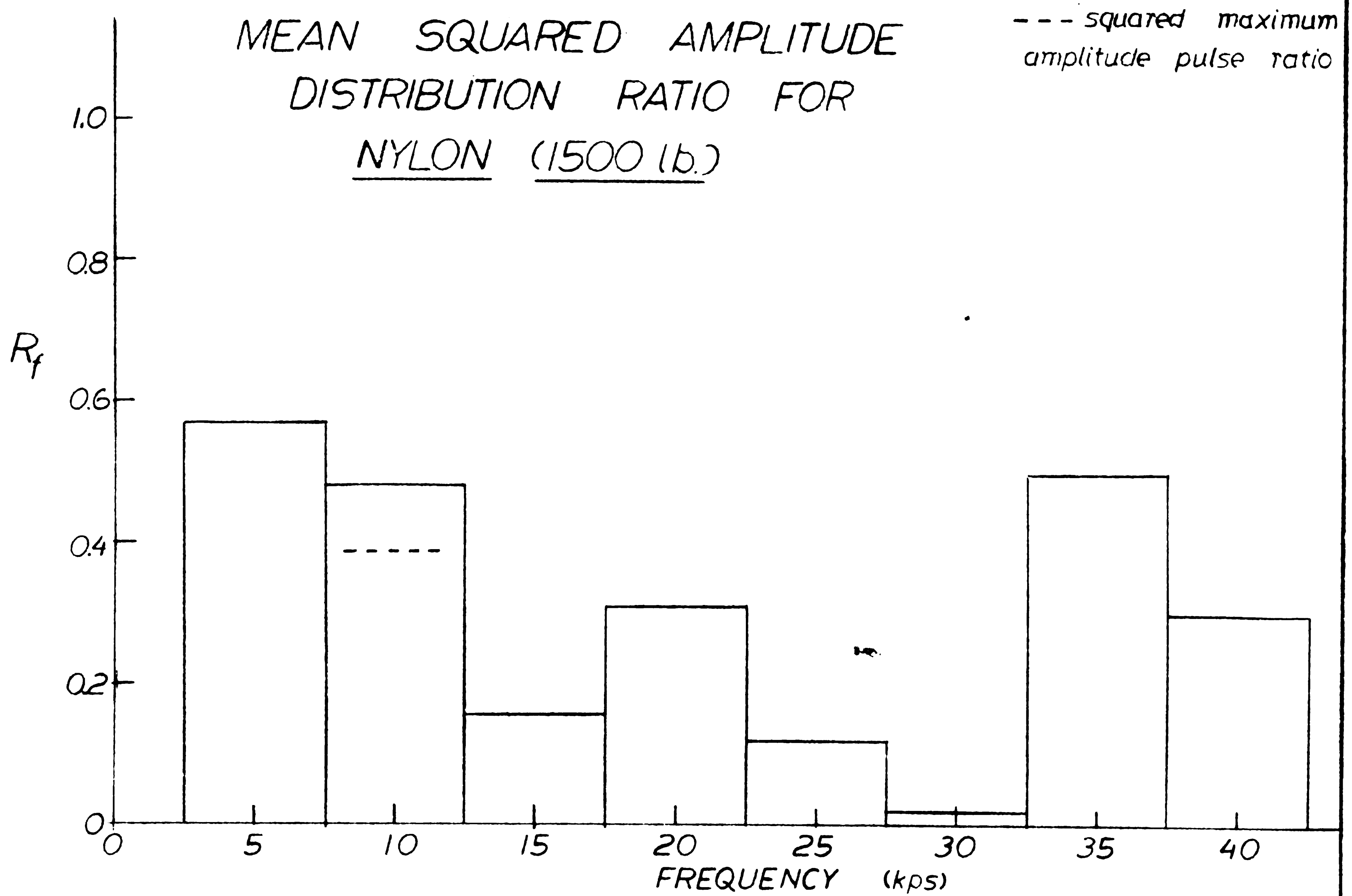

FIGURE 17

MEAN SQUARED AMPLITUDE DISTRIBUTION RATIO FOR NYLON (4000 lb.)

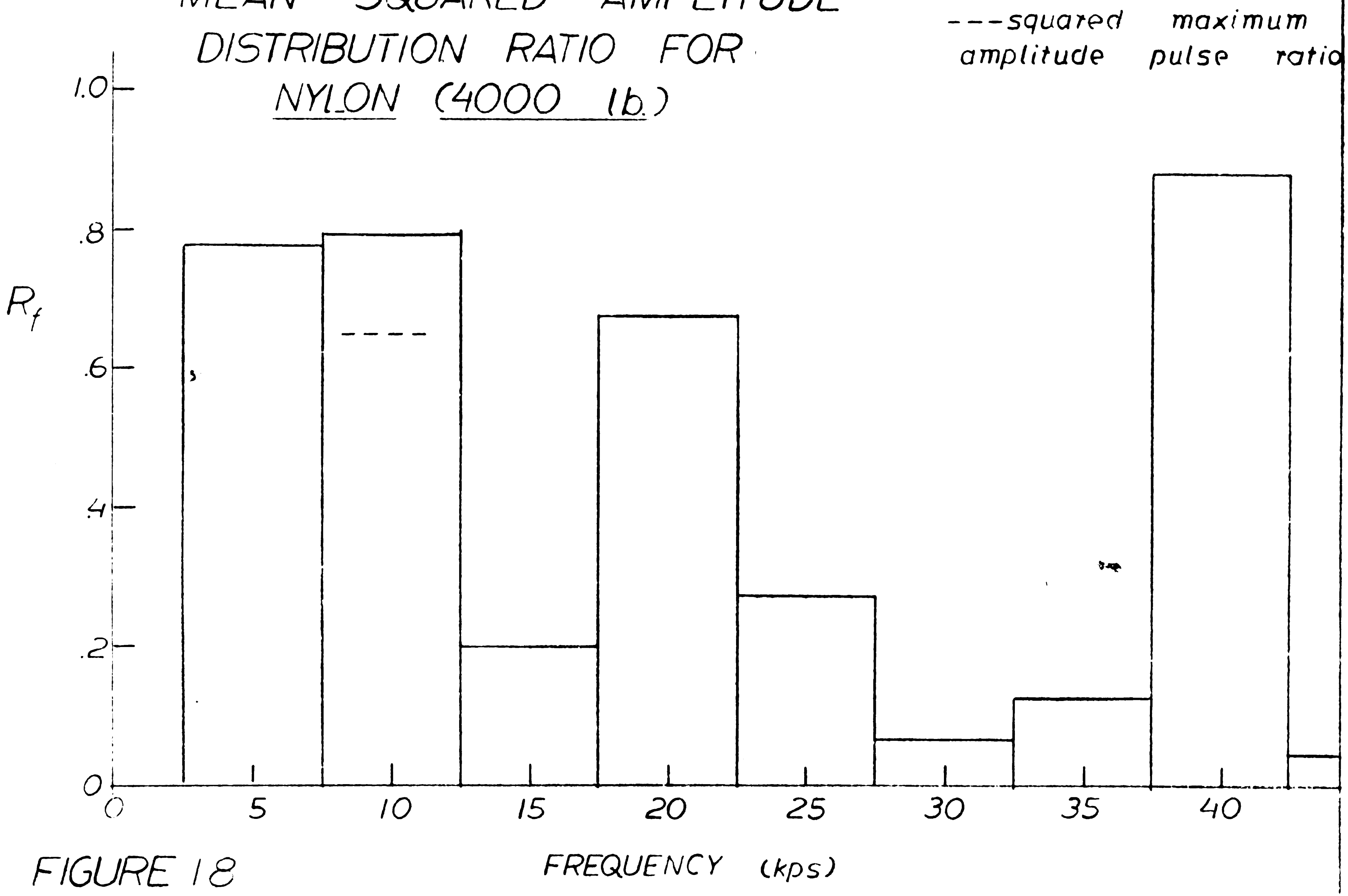

FIGURE 18

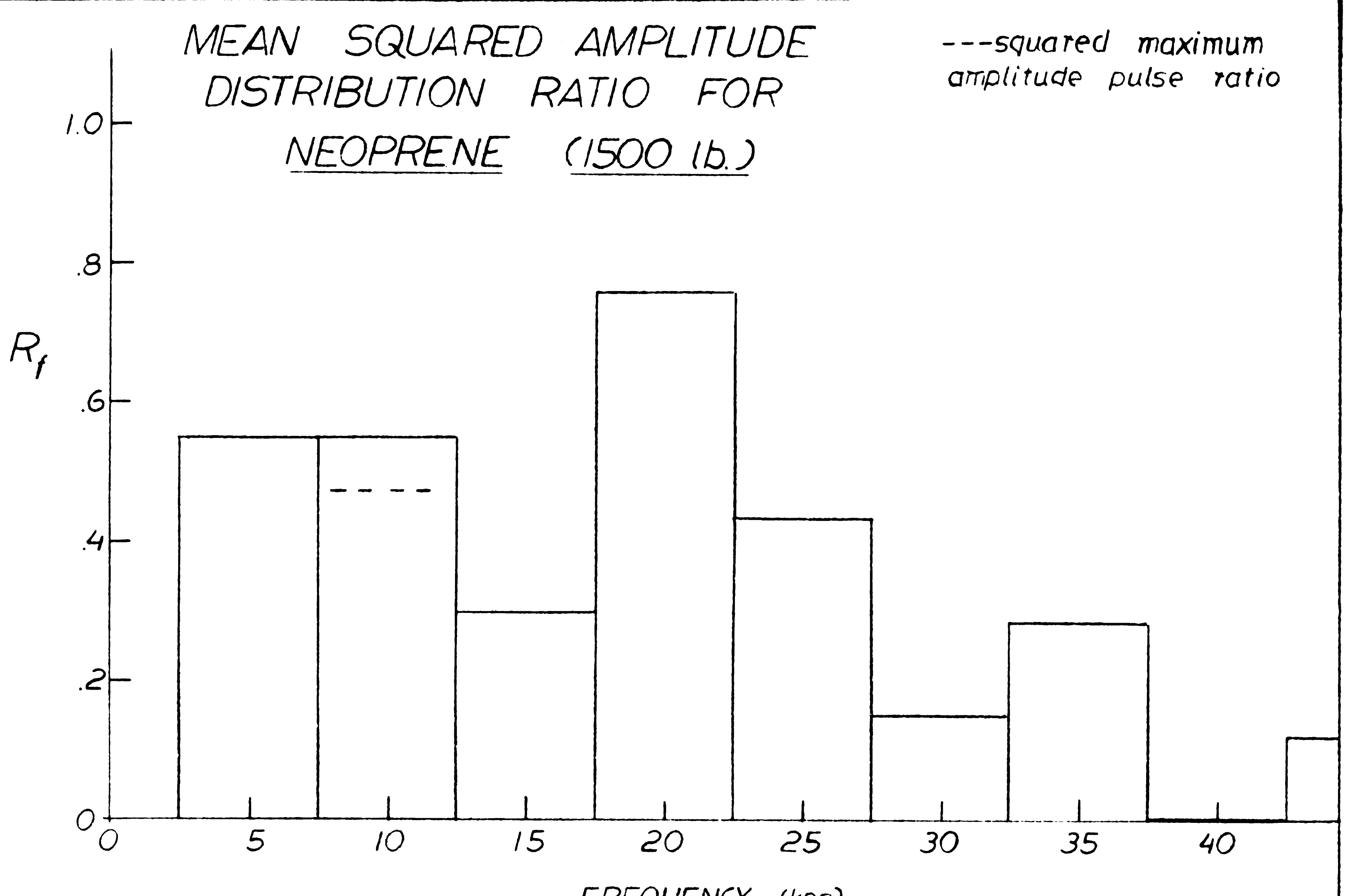

MEAN SQUARED AMPLITUDE DISTRIBUTION RATIO FOR NEOPRENE (1500 lb.)
---squared maximum amplitude pulse ratio
1.0
.8
.6
.4
.2
0
R_f
0
5
10
15
20
25
30
35
40
FREQUENCY (kps)

FIGURE 19

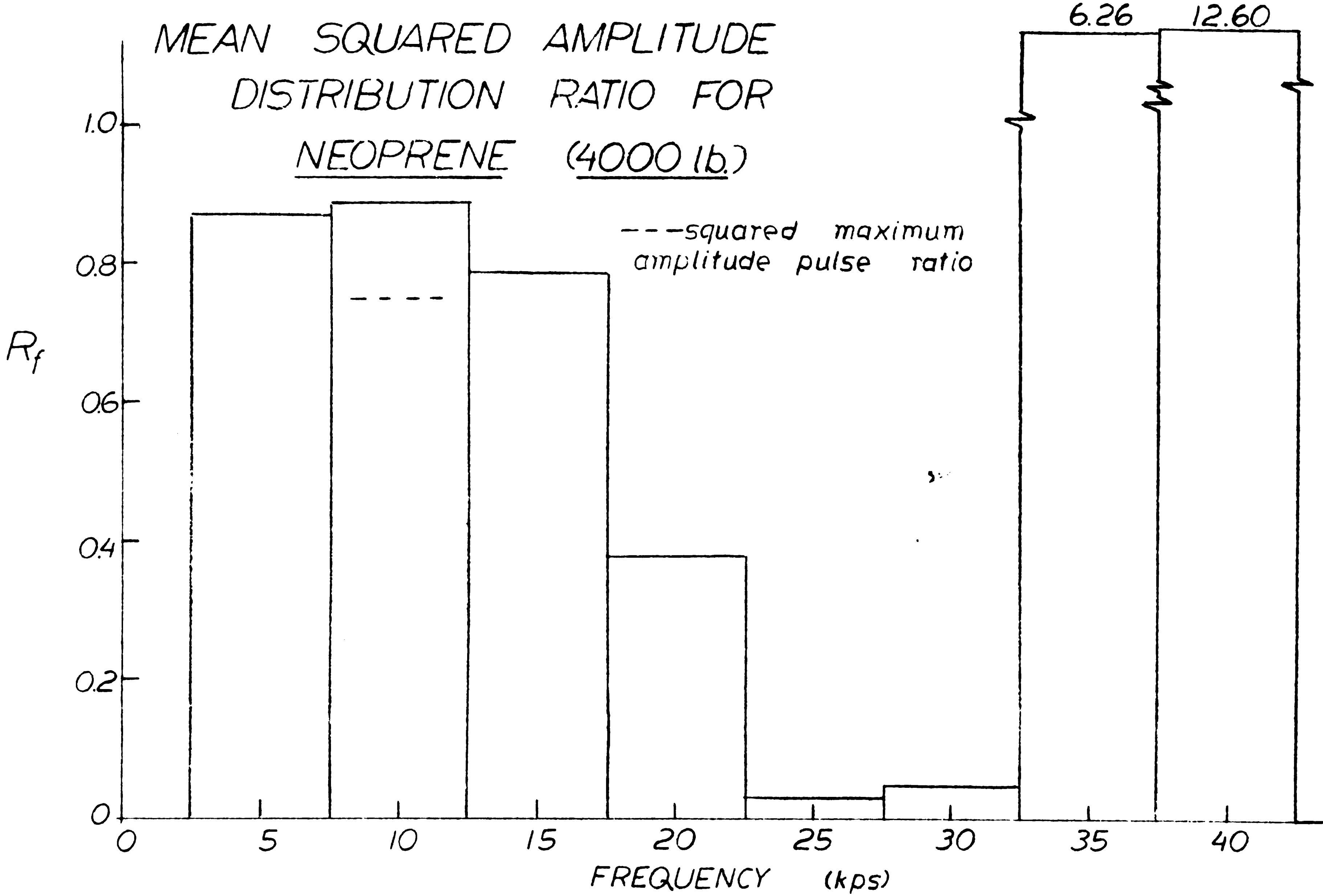
MEAN SQUARED AMPLITUDE
DISTRIBUTION RATIO FOR
NEOPRENE (4000 lb.)
---squared maximum
amplitude pulse ratio
6.26
12.60
R_f
1.0
0.8
0.6
0.4
0.2
0
0
5
10
15
20
25
30
35
40
FREQUENCY (kps)

FIGURE 20

CHAPTER IV

RESULTS AND CONCLUSIONS

The results of this investigation are the mean squared amplitude distribution ratio histograms (shown in Figures 15-20). These graphs give a qualitative view of the energy loss (or gain) as a function of frequency.

The first thing to be noticed from these graphs is that for the lower loads there is less energy transmission than for the higher loads. This would be expected since for a higher load the specimen becomes more compressed and the acoustic resistance comes closer to matching the acoustic resistance for the steel. As was stated in the introduction, if the acoustic resistances are well matched than there will be better energy transmission (poorer sound isolation).

From looking at the two histograms for white felt at 4000 lbs. and 1500 lbs., it is seen that the maximum ratios occur at the same frequency bands (20 kps and 40 kps) and that the general shapes of these two histograms are almost proportional in form to each other, the 1500 lb load histogram naturally being proportionally smaller for all values.

The same effect is noticed from the histograms for nylon, but the correlation is not quite as good as for the white felt. The two histographs for neoprene show no such correlation. Therefore it could be said that for materials which are not rubbery (such as white felt) the mechanical properties are not a function of the stress which is applied. But for materials which are rubber-like the mechanical properties are a function of the stress. The degree of dependence on the stress is somewhat related to the degree of rubberiness, for instance nylon is much less rubber-like than neoprene.

It is also seen from these histograms that some of the ratios are more than one. This is not hard to justify heuristically if one thinks of the effects which cause this phenomenon to be analogous to the factors causing resonance in a vibrating system.

On the same graphs as the histograms can be seen the ratio of the squared maximum amplitudes of the output to input pulses plotted at the fundamental frequency of the input pulse. One sees that these values fall fairly close to the mean squared amplitude distribution ratios at the fundamental frequency. Therefore if one wished to obtain a rough measure of the energy transmission at the fundamental frequency it could be obtained by taking the ratios of the squared maximum amplitudes of the output to input pulses. But for values at higher frequencies it would be necessary to go through the complete mathematical procedure described.

It should be noted that an assumption has to be made in order to justify the use of the Fourier analysis which has been used. The Fourier analysis requires a linear system (perfectly elastic) for the superposition principle to be valid. This assumption then is that the materials we are dealing with are perfectly elastic. This assumption would be completely erroneous, obviously, for the materials being used (neoprene, nylon, etc.) except for the fact that the strains caused by the stress wave are of very small magnitude (150 μin/in). Since, even though a material may have a nonlinear stress-strain curve, the portion in the neighborhood of the static stress can be assumed to be linear with not too great an error.

Because of the above assumption any wave can be obtained by a simple superposition (a linear combination) of separate monochromatic waves, each of which is propagated independently and which do not intersect with one another. However, these properties no longer hold if the nonlinearities of the specimen are very pronounced.

The effects which appear due to the nonlinearities, though small, may be of importance in certain phenomena. These effects are usually called "anharmonic effects", since the corresponding equations of motion are nonlinear and do not have simple periodic (harmonic) solutions.

These anharmonic effects will now be discussed. It has been shown (La 59) that the superposition of two monochromatic waves satisfying certain conditions (relations between their frequency and wave vectors) leads to resonance. In other words a new monochromatic wave is formed, whose amplitude increases with time and eventually is no longer small. This anharmonic effect involving resonance occurs not only when several monochromatic waves are superposed, but also when there is only one wave. From the single monochromatic wave there may result (if the frequency and wave vector satisfy certain conditions) besides this original wave, waves with twice the frequency and the amplitude increasing with time.

These anharmonic effects are most probably the reason for ratios being more than one in the mean squared amplitude distribution histograms of some of the specimens.

The results of this study could be checked by using different lengths of striker bars (therefore different pulse shapes) on the same materials under the same conditions. The data obtained should all be fairly close to those obtained here.

Another field of investigation in connection with this study would be to see what correlation existed between these results and results obtained using input excitation composed of a single frequency. In other words using steady state inputs, at various frequencies, on materials statically compressed.

BIBLIOGRAPHY

(Au 61) Auberger, M. and Rinehart, J. S., "Ultrasonic Attenuation of Longitudinal Waves in Plastics," J. Appl. Phys., Vol. 32, 1961, p. 219.

(Ba 44) Ballou, J. W. and Silverman, S., "Young's Modulus of Fibers and Films by Sound Velocity," J. Acoust. Soc. Amer., Vol. 16, 1944, p. 113.

(Ba 49) Ballou, J. W. and Smith, J. C., "Dynamic Measurements of Polymer Physical Properties," J. Appl. Phys., Vol. 20, 1949, p. 493.

(Hi 49) Hillier, K. W., "The Measurement of Dynamic Elastic Constants," Proc. Phys. Soc. B, Vol. 62, 1949, p. 701.

(Hi K 49) Hillier, K. W. and Kolsky, H., "Dynamic Elastic Properties of Some High Polymers," Proc. Phys. Soc. B, Vol. 62, 1949, p. 111.

(Hu 49) Hughes, D. S., Pondrom, W. L. and Mims, R. L., "Transmission of Elastic Pulses in Metal Rods," Phys. Rev., Vol. 63, 1949, p. 1552.

(Iv 49) Ivey, D. G., Mrowca, B. A. and Guth, E., "Propagation of Ultrasonic Bulk Waves in High Polymers," J. Appl. Phys., Vol. 20, 1949, p. 486.

(Ko 53) Kolsky, H., Stress Waves in Solids, London: Oxford University Press, 1953, p. 91.

(La 59) Landau, L. D. and Lifshitz, E. M., Theory of Elasticity. Translated from the Russian by J. B. Sykes and W. H. Reid, London: Pergamon Press, 1959.

(Li 60) Lindsay, R. B., Mechanical Radiation, New York: McGraw Hill Book Company, 1960, p. 77.

(No 48) Nolle, A. W., "Dynamic Mechanical Properties of Rubber-Like Materials," J. Polymer Sci., Vol. 5, 1959, p. 1.

(Ta 60) Tatro, C. A., "Acoustic Emission from Crystalline Materials Subjected to External Loads," Division of Engineering Research, College of Engineering, Michigan State University, 1960.

(Wh 54) Whittaker, E. and Robinson, G., The Calculus of Observations, London: Blackie and Son Limited, 1954, p. 263.

APPENDIX

CALCULATION OF THE FOURIER INTEGRAL TRANSFORM (AMPLITUDE DISTRIBUTION FUNCTION)

Using the well known formulae,

$$F(t) = \int_0^{\infty} A'(\omega) \sin \omega t \, d\omega$$

$$A'(\omega) = \frac{2}{\pi} \int_0^{\infty} F(t) \sin \omega t \, dt$$

and Figure 7

$$F(t) = \begin{cases} f(t) & 0 \leq t \leq L \\ 0 & L \leq t < \infty \end{cases}$$

one gets

$$A'(\omega) = \frac{2}{\pi} \int_0^{L} f(t) \sin \omega t \, dt \quad .$$

From Eq. (1)

$$A'(\omega) = \frac{2}{\pi} \int_0^{L} \left(\sum_{i=1}^{6} b_i \sin \frac{i \pi t}{L} \right) \sin \omega t \, dt$$

Since the functions are continuous the order of summation and integration can be interchanged. Therefore,

$$A'(\omega) = \frac{2}{\pi} \sum_{i=1}^{6} b_i \int_0^{L} \sin \frac{i \pi t}{L} \sin \omega t \, dt$$

For convience let

$$a_i = \frac{i \pi}{L}$$

Then integrating by parts one obtains

$$A'(\omega) = 2\,L \sin \omega L \sum_{i=1}^{6} \frac{b_i (-1)^i\, i}{(\omega L)^2 - (i\pi)^2}$$

Changing to frequency units of cycles/unit time

$$\omega = 2\,\pi\, f$$

then

$$A(f) = A'(2\pi f) = 2L \,\frac{\sin(2\pi f L)}{\pi^2} \sum_{i=1}^{6} b_i \frac{(-1)^i\, i}{4\,(fL)^2 - i^2} \tag{3}$$

Eq. (3), as it stands, looks pretty frightening to plot, so it will now be simplified in order to see the behavior of the function A(f). First it is seen that when $f = \frac{i}{2L}$ all the terms drop out except the i^{th} term; since in this term the denominator goes to zero and there is an indeterminate form of $\frac{0}{0}$. So using L'Hospital's rule,

$$A(\tfrac{i}{2L}) = \frac{2L}{\pi^2}\, b_i\, (-1)^i\, i \lim_{f \to \frac{i}{2L}} \frac{\sin 2\pi L f}{4L^2 f^2 - i^2}$$

$$= \frac{2L}{\pi^2}\, f_i\, (-1)^i\, i \lim_{f \to \frac{i}{2L}} \frac{2\pi L \cos 2\pi L f}{8\,L^2\, f}$$

$$= \frac{b_i L}{\pi} \tag{4}$$

From Eq. (4) six values of A(f) are immediately known at

$$f = \frac{1}{2L}\,,\ \frac{2}{2L}\,,\ \ldots\ \frac{6}{2L}$$

Another simplification of Eq. (4) is obtained when

$$f = \frac{2m - 1}{4L}, \quad m = 1, 2 \ldots\ldots 6$$

so that

$$A\left(\frac{2m-1}{4L}\right) = \frac{2L}{\pi^2}(-1)^{m+1} \sum_{i=1}^{6} \frac{b_i(-1)^i\, i}{\left[m^2 - m + \frac{1}{4}\right] - i^2} \tag{5}$$

Eq. (5) can be put in the form of a matrix equation to facilate computation

$$A_m = \frac{2L}{\pi^2}(-1)^{m+1}\, B_{mi}\, b_i \qquad \begin{matrix} i = 1, 2, \ldots\ldots 6 \\ \\ m = 1, 2, \ldots\ldots 6 \end{matrix} \tag{6}$$

Where B_{mi} is a six by six matrix and b_i is a six element column matrix.

By observing Eq. (5) it is seen that B_{mi} is the same for any set of b_i's. Therefore one can look at B_{mi} as a transformation matrix which transforms the coefficients of a finite Fourier series into values of the amplitude distribution function (Fourier transform).

Eq. (6) gives six more values of A(f) equally spaced between those given by Eq. (4). So with Eqs. (4) and (6) enough information is given to see how the function A(f) behaves.